

## Characterization and Prebiotic Activity *in Vitro* of Hydrolyzed Glucomannan Extracted from Fresh Porang Tuber (*Amorphophallus Oncophyllus*)

Rani Satiti<sup>1</sup>, Tyas Utami<sup>1</sup>, Jaka Widada<sup>2</sup> and Eni Harmayani<sup>1,\*</sup>

<sup>1</sup>Department of Food and Agricultural Product Technology, Faculty of Agricultural Technology, Universitas Gadjah Mada, Yogyakarta 55281, Indonesia

<sup>2</sup>Department of Microbiology, Faculty of Agriculture, Universitas Gadjah Mada, Yogyakarta 55281, Indonesia

(\*Corresponding author's e-mail: eniharmayani@ugm.ac.id)

Received: 28 June 2024, Revised: 26 July 2024, Accepted: 2 August 2024, Published: 10 November 2024

### Abstract

The technology for direct extraction of porang glucomannan (PG) from fresh tubers offers a faster and simpler process, yielding high-purity glucomannan. However, PG's high viscosity and low solubility limit its use in the food, pharmaceutical, and health industries. Enzymatic hydrolysis of PG has the potential to improve these characteristics and enhance its prebiotic activity. This study aimed to examine the characteristics and prebiotic activity of porang glucomannan hydrolysate (PGH) derived from glucomannan extracted directly from the fresh tubers. PG was hydrolyzed under optimal conditions at 37.6 °C for 3 h, pH of 6.8, and an E/S of 0.8 % (w/w). Analysis of PGH included the degree of polymerization (DP), molecular weight (MW), viscosity, and solubility. Changes in the morphology, molecular structure, and composition of PGH were assessed through scanning electron microscopy (SEM), Fourier-transform infrared spectroscopy (FTIR), and high-performance liquid chromatography (HPLC), respectively. Prebiotic activity analysis was conducted by determining the prebiotic activity score *in vitro*. The results revealed that PGH was composed of 58 % mannohexaose, 40 % mannotriose, and 2 % mannobiose. Notably, PGH exhibited reduced granule size and a porous surface. FTIR analysis indicated a structural change in the PGH molecule after hydrolysis. The DP of PG decreased by 1000 times, and the MW decreased by 60 times, leading to a 700-fold reduction in the viscosity of PGH. In contrast, the solubility of PGH increased threefold, attributed to the disruption of glycosidic and hydrogen bonds between and within glucomannan molecules during hydrolysis. These modifications in PGH characteristics make it more readily fermentable by several Lactobacilli and Bifidobacteria without stimulating the growth of *E. coli*, resulting in a positive prebiotic activity score. As a result, PGH shows promise as a source of prebiotics and can be utilized in beverage products to enrich their nutritional value, consequently producing functional food.

**Keywords:** Porang glucomannan (PG), Porang glucomannan hydrolysate (PGH), Enzymatic hydrolysis, Characteristics, Prebiotic activity score

### Introduction

Glucomannan is a neutral polysaccharide composed of mannose and glucose residues linked by  $\beta$ -1, 4 glycosidic bonds with a mannose: Glucose ratio varying from 1.5:1 to 4.2:1 depending on the origin of glucomannan. Some residues in glucomannan are acetylated, which promotes solubility and dispersion [1,2]. The most commonly marketed glucomannan is konjac glucomannan (KG), produced from konjac

tubers (*Amorphophallus konjac*). Recently, glucomannan from porang tubers (*Amorphophallus oncophyllus*) has been produced in Indonesia [3].

Glucomannan exhibits extraordinary water-holding capacity, forming a highly viscous solution when dissolved in water [4,5]. This makes glucomannan widely used as a food additive for fat replacements, emulsifiers, stabilizers, thickeners, and gel formers [6-

8]. Research has shown that it may offer several health benefits, including anti-obesity, anti-inflammatory, immunomodulatory, and prebiotic activity [3,9-11].

Glucomannan can be extracted through a mechanical dry process or a wet process using chemicals [12]. Several studies have modified the extraction process to produce highly pure glucomannan by combining dry and wet processes. The dry process is carried out by slicing the tubers, drying them into chips, and grinding them into flour, followed by sieving and air purification [13]. However, this process produces crude flour with low purity because drying the tubers into chips will cause them to harden so that impurities stick more to the glucomannan granules and are difficult to remove [14]. Therefore, further purification using a wet process is necessary. Previous studies have carried out a wet process to purify crude flour by stirring in 50 % ethanol followed by centrifugation, evaporation, overnight precipitation with 95 % ethanol at 4 °C, washing, filtration, freeze drying, and milling [12]. The process was long, required a significant amount of equipment, and consumed large quantities of ethanol. Another study used  $\alpha$ -amylase to remove starch impurities from crude flour, but the purity of the glucomannan produced was still less than 90 % [15].

Recently, Yanuriati *et al.* [14] discovered a new technology for directly extracting glucomannan from fresh porang tubers. This method is more efficient as it eliminates the need to process the tubers into chips and crude flour, resulting in a shorter process that involves only repeated milling in ethanol followed by filtration without additional purification. This new process yields PG with a purity of up to 90.98 %, low amounts of ash and protein, no detectable starch, and the appearance of white glucomannan granules. However, PG has lower solubility and higher viscosity compared to glucomannan extracted from crude porang flour, thus limiting its application in the food, pharmaceutical, and health industries [16,17].

Efforts to enhance the solubility of PG and reduce its viscosity through modification processes are crucial for its optimal utilization as a functional food ingredient. One effective method involves enzymatic hydrolysis, mainly using  $\beta$ -mannanase, due to its high efficiency, ease of operation, and mild reaction conditions [18]. This hydrolysis process simplifies the structure of glucomannan, thereby influencing its prebiotic potential

[19,20]. Previous studies have conducted the hydrolysis of PG obtained from a combined extraction process [21-23]. However, the characteristics of the resulting hydrolysate products have not been identified. Therefore, this study aims to examine the characteristics of PGH hydrolyzed from PG extracted from fresh porang tubers using  $\beta$ -mannanase and analyze its prebiotic activity *in vitro*.

## Materials and methods

### Materials and chemicals

The materials used for PG extraction were 2-years-old fresh porang tubers (*Amorphophallus oncophyllus*) with a weight ranging from 1000 - 2000 g obtained from Nglanggeran Village, Gunung Kidul, Indonesia, ethanol 96 %, and aquadest. The materials used for the hydrolysis of PG were  $\beta$ -mannanase (Mianyang Habio Bioengineering Co. Ltd.) and phosphate-citrate buffer. De Man, Rogosa, and Sharpe Agar and Broth (MRSA and MRSB) and Nutrient Agar and Broth (NA and NB) were purchased from Merck KGaA, Darmstadt, Germany, and Thermo Scientific Oxoid, USA, respectively. Bacterial strains, including *Lactobacillus acidophilus* FNCC 0051, *Lactobacillus plantarum* FNCC 0020, *Bifidobacterium longum* FNCC 0210, *Bifidobacterium bifidum* FNCC 0211 and *Escherichia coli* FNCC 0091 were from the Food and Nutrition Culture Collection (FNCC) Center for Food and Nutrition Studies, Universitas Gadjah Mada, Yogyakarta, Indonesia. Inulin was purchased from Beneo Orafiti, Tienen, Belgium. All other analytical-grade chemicals were purchased from Merck KGaA, Darmstadt, Germany.

### The technology for directly extracting PG from fresh porang tubers

PG was extracted from fresh porang tubers using the method described by Yanuriati *et al.* [14] with slight modifications. The tubers were peeled, washed, and cubed before being milled in a 50 % ethanol solution (tuber-to-ethanol ratio of 1:1.75) for 5 min at 12,000 rpm. The resulting mixture was filtered to obtain crude glucomannan. This process was repeated 7 times to obtain glucomannan granules. The granules were then dried in a vacuum dryer at 50 °C until the water content reached  $\leq 10$  %. The obtained PG was stored in an air-tight container at room temperature for future use.

### Hydrolysis of PG

The hydrolysis of PG was conducted using the previously determined optimal conditions (data not shown). Two g of PG was added to 200 mL of phosphate-citrate buffer (pH 6.81) and then mixed with  $\beta$ -mannanase (E/S ratio of 0.8 %, w/w) to start the hydrolysis. The mixture was incubated for 3 h, and the water bath temperature was kept steady at 37.6 °C. The hydrolysis was terminated by boiling the mixture for 15 min. The sample was then vacuum-filtered, and the filtrate was spray-dried to produce PGH powder. PGH was stored in an air-tight container at 4 °C for further analysis.

### Morphology

The morphology of PG or PGH was analyzed using a Scanning Electron Microscope (SEM) [14]. The dried sample was placed in an auto coater (JEC-3000FC, JEOL, Japan) at a pressure of  $\pm 3.2$  Pa for approximately 2 min. The sample was then put into an SEM (JSM-6510LA, JEOL, Japan) and vacuumed for  $\pm 1$  min. The sample was shot with electrons with a certain-level probe, and then the surface topography of the sample was observed.

### Fourier transform infrared (FTIR) spectroscopy

The FTIR spectra of PG and PGH were recorded on a Nicolet iS10 FTIR spectrometer (Thermo Scientific, USA). One mg sample was ground with 100 mg potassium bromide (KBr) and pressed onto disks for scanning in the wavenumber range 4000 - 400  $\text{cm}^{-1}$  at a resolution of 4  $\text{cm}^{-1}$  with 128 co-added scans [24].

### Degree of polymerization

The degree of polymerization (DP) of PG and PGH was calculated as the ratio of the total reducing sugar (TRS) to direct reducing sugar (DRS). The analysis for TRS involved the phenol-sulphuric acid method with glucose as the standard, while the Somogyi method was used for DRS. The DP was calculated by dividing TRS by DRS with the formula  $DP = TRS/DRS$  [25].

### Molecular weight

The molecular weight (MW) analysis of PG and PGH refers to Ratcliffe *et al.* [26] with slight modifications. The prepared sample (10  $\mu\text{L}$ ) was injected into gel permeation chromatography (HLC-8320GPC, TOSOH, Japan) equipped with a TSKgel SuperAW5000 column (TOSOH, Japan) and RI detector (TOSOH, Japan). The mobile phase was deionized water with a flow rate of 0.35 mL/min, and the column and detector temperature was 40 °C. Analyses were processed using the software package (GPC Workstation EcoSEC-WS).

### Apparent viscosity

The apparent viscosity of PG and PGH was calculated using the method described by Yanuriati *et al.* [14] with modification. 1 g of sample was dissolved in 100 mL of distilled water at 40 °C until completely hydrated. The sample was then tested for viscosity by Brookfield Viscometer Model RVT at room temperature with spindle no.3 at 0.5 rpm.

### Solubility

The analysis of solubility refers to Du *et al.* [27]. 0.1 g of PG or PGH was dissolved in 24.9 g of deionized water and agitated for 1 h at room temperature. The mixture was centrifuged at 4000 rpm for 20 min at room temperature, then the supernatant ( $\pm 10$  g) was dried to constant weight at 105 °C. The solubility was calculated with the following equation:

$$\text{Solubility \%} = \frac{m \times 2.5}{w} \times 100 \% \quad (1)$$

where  $m$  is the weight of the soluble components in 10 g upper solution, and  $w$  is the overall weight of the sample.

### Oligosaccharides analysis of PGH

Oligosaccharides of PGH were analyzed following the method described by Rungruangsaphakun *et al.* [28] with slight modification using high-performance liquid chromatography (HPLC; Shimadzu, Japan) equipped with an Aminex HPX-87H column (Bio-Rad, USA) and a refractive index detector (Shimadzu, Japan). The mobile phase of the experiment consisted of deionized water with a flow rate of 0.4

mL/min, a column temperature of 60 °C, a detector temperature of 40 °C, and an injection volume of 20 µL. A variety of standard sugar solutions, including glucose, mannose (M1), mannobiose (M2), mannotriose (M3), mannotetraose (M4), mannopentaose (M5), and mannohexaose (M6) (Megazyme, Ireland) were used for calibration. The samples were diluted to achieve concentration within the range calibration curve of the standard reference [23].

### Prebiotic activity assay *in vitro*

Prebiotic activity assay was done by calculating the prebiotic activity score reported by Huebner *et al.* [29]. Bacterial pure cultures were stored at -20 °C in a 10 % skim milk solution [30]. Under sterile conditions, 0.5 mL frozen stock culture of Lactobacilli and Bifidobacteria were inoculated into 10 mL sterilized MRS broth medium, while nutrient broth medium was used for *E. coli*. For Bifidobacteria, 0.05 % L-cysteine HCl was added to the MRS broth. Lactobacilli and *E. coli* were incubated under aerobic conditions at 37 °C for 24 h, while Bifidobacteria were incubated under anaerobic conditions at 37 °C for 24 h.

The assay was conducted by adding 1 % (v/v) of activated cultures into separate mediums containing 2 % (w/v) glucose, PG, PGH, or inulin. The cultures were incubated at 37 °C for 24 h in anaerobic conditions for Bifidobacteria, and under ambient atmosphere for all other strains. The anaerobic condition was prepared by placing the anaerobic gas pack (Anaerogen TM, Thermo Scientific Oxoid, USA) in an anaerobic chamber. At 0 and 24 h, the inoculated samples were enumerated by serial dilution and pour plate method on MRS agar (Lactobacilli and Bifidobacteria) or nutrient agar medium (*E. coli*). Each assay was repeated at least 3 times, and the results were calculated as colony-forming units per milliliter (CFU mL<sup>-1</sup>). The prebiotic activity score was determined using the following equation:

Prebiotic activity score =

$$\frac{\left[ \frac{\text{probiotic log CFU mL}^{-1} \text{ on the prebiotic at 24 h} - \text{probiotic log CFU mL}^{-1} \text{ on the prebiotic at 0 h}}{\text{probiotic log CFU mL}^{-1} \text{ on the glucose at 24 h} - \text{probiotic log CFU mL}^{-1} \text{ on the glucose at 0 h}} \right] - \left[ \frac{\text{enteric log CFU mL}^{-1} \text{ on the prebiotic at 24 h} - \text{enteric log CFU mL}^{-1} \text{ on the prebiotic at 0 h}}{\text{enteric log CFU mL}^{-1} \text{ on the glucose at 24 h} - \text{enteric log CFU mL}^{-1} \text{ on the glucose at 0 h}} \right]}{2} \quad (2)$$

A positive prebiotic activity score will be obtained when the given carbon source can support the growth of probiotic bacteria as well as glucose and can be metabolized selectively by the probiotic strain but not by other intestinal bacteria. A higher score indicates higher prebiotic activity [31].

### Statistical analysis

Data of experiments are presented as mean ± standard deviation. A paired t-test was used to determine any significant differences in the characteristics of PG and PGH. Additionally, one-way ANOVA followed by Duncan's new multiple-range tests was used to assess any significant differences in the increase of viable cells for each carbon source treatment of a given strain and the prebiotic activity score. SPSS software (Version 26) was utilized to perform these statistical analyses, with a significance level of  $p < 0.05$ .

## Results and discussion

### Morphology of PG and PGH

The morphological changes of PG and PGH before and after enzymatic hydrolysis were examined using SEM. Initially, PG granules exhibited a round oval shape with a dense, rough, and scale-like surface (**Figures (A) - (C)**). This scale-like surface was attributed to the cell wall attached to the glucomannan granules [14]. Following enzymatic hydrolysis, the PG granules were disrupted, resulting in an irregular shape (**Figures (D) - (F)**). Additionally, numerous cavities appeared on the granule surface, and the granules were no longer as dense as PG. The surface of PGH granules appeared smoother, indicating the release of the previously attached cell wall during the hydrolysis process. These findings suggest that the enzymatic hydrolysis process was effective in breaking the hydrogen bonds in the glucomannan chain, leading to the destruction of the granules and erosion of the PGH granule surface [18,32].

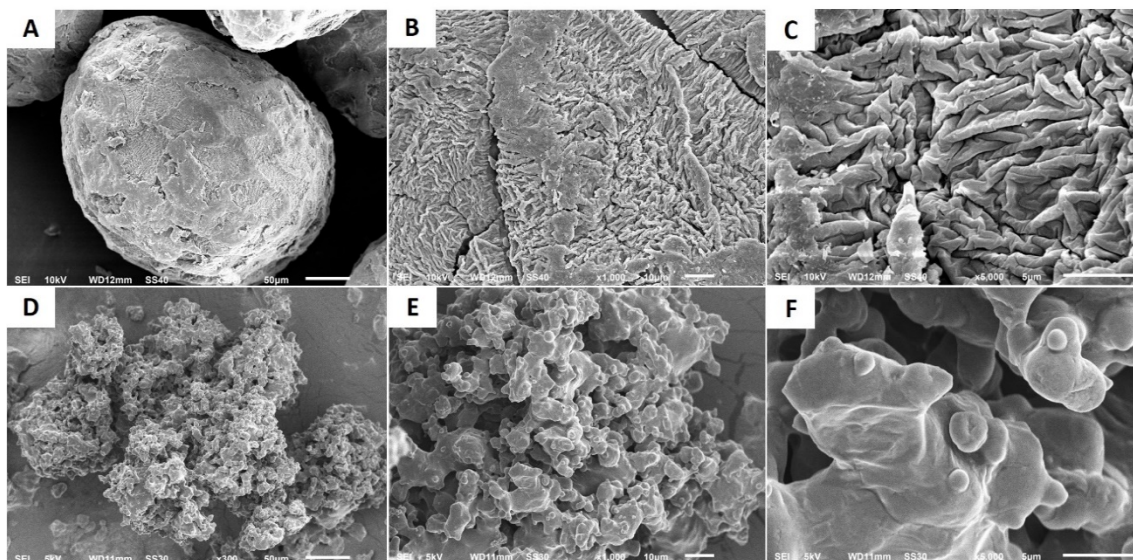


**Figure 1** SEM images of PG before hydrolysis (A–C) and PGH after the hydrolysis process using  $\beta$ -mannanase (D–F) with 300 $\times$ , 1000 $\times$ , and 5000 $\times$  magnifications (from left to right).

### FTIR analysis

FTIR is a rapid and effective method for identifying molecular structures [33,34]. This technique monitors the bending and stretching vibrations of chemical bonds as they absorb infrared radiation, enabling the detection of specific functional groups based on their characteristic absorption peaks [35]. FTIR spectra of PG and PGH are shown in **Figure 2**. The broad peaks at approximately 3400  $\text{cm}^{-1}$  in both PG and PGH were due to the stretching vibration of O–H groups [36]. The peak observed at 2939  $\text{cm}^{-1}$  for the stretching vibration of the C–H bond in the methyl group, along with the peak at 1734  $\text{cm}^{-1}$  for the carbonyl, were attributed to the acetyl groups in the PG [37]. The peaks at 1636  $\text{cm}^{-1}$  (PG) and 1589  $\text{cm}^{-1}$  (PGH) were attributed to the C=O asymmetric stretching vibration of the carboxylate groups [11]. Furthermore, the peaks at 1396  $\text{cm}^{-1}$  and 1069  $\text{cm}^{-1}$  in PGH, and 1048  $\text{cm}^{-1}$  in PG were caused by the stretching vibration of the methylene groups [38]. Lastly, the small peaks detected around 800  $\text{cm}^{-1}$  in both PG and PGH were associated with mannose [39].

The hydrolysis process increased the peak intensity of the O–H group in PGH. This effect was due to the cutting of long chains of glucomannan by  $\beta$ -mannanase, which produced more hydroxyl radicals [40]. Enzymatic hydrolysis also led to significant changes in PG undergoing degradation, resulting in the disappearance of peaks around 2900 and 1700  $\text{cm}^{-1}$ , indicating deacetylation [41]. The peak of mannose around 800  $\text{cm}^{-1}$  also exhibited weaker intensity in PGH. Furthermore, significant changes were observed in the major peaks between 1800 - 1000  $\text{cm}^{-1}$ , with some peaks either shifting or disappearing after hydrolysis. The findings in this study differ slightly from previous study that utilized  $\beta$ -mannanase for KG hydrolysis [18]. In the previous study, the peak around 3400  $\text{cm}^{-1}$  became narrower, while the peaks at 2900 and 1700  $\text{cm}^{-1}$  decreased in intensity, but did not disappear as they did in this study. This suggests that enzymatic hydrolysis of different substrates causes distinct changes in the molecular structure.

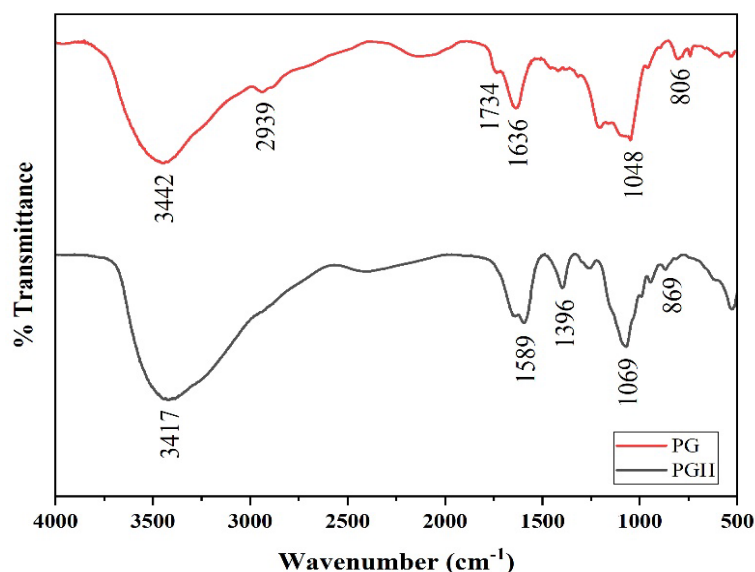


**Figure 2** FTIR spectra of PGM and PGH.

### Changes in DP and MW

It is essential to determine the DP and MW of PG degradation products through enzymatic hydrolysis, as it plays a significant role in affecting the viscosity, solubility, and prebiotic potential of glucomannan [18,42]. The DP and MW of PG and PGH are shown in **Table 1**. The initial DP of PG was measured at  $5394.45 \pm 153.04$ , but after the hydrolysis process, it decreased significantly by approximately 1000-fold to  $5.15 \pm 0.16$ , indicating a successful hydrolysis process. This finding aligns with a study by Liu *et al.* [11], which revealed a DP of 5.2 for KOG after KG hydrolysis. However, it differs slightly from the study by Anggela *et al.* [23],

which involved PG hydrolysis from porang flour and yielded a hydrolysate product with a DP value of 3.

Similar to DP, the MW of PG also significantly decreased by nearly 60-fold, dropping from  $1326.66 \pm 20.30$  kDa to  $23.38 \pm 5.45$  kDa. Previous studies demonstrated that enzymatic hydrolysis can substantially decrease the MW of glucomannan, with reductions ranging from 40 to 500 times depending on the concentration of the enzyme and the duration of the hydrolysis process [18,37,43]. These findings suggest that enzymatic hydrolysis cleaved the glycosidic bonds of PG and disrupted its molecular structure [18,38], as evidenced by the SEM results showing damaged granule surfaces of PGH (**Figure 1**).

**Table 1** The degree of polymerization (DP), molecular weight (MW), apparent viscosity, and solubility of PG and PGH.

|                          | PG                     | PGH                |
|--------------------------|------------------------|--------------------|
| Degree of polymerization | $5394.45 \pm 153.04^a$ | $5.15 \pm 0.16^b$  |
| Molecular weight (kDa)   | $1326.66 \pm 20.30^a$  | $23.38 \pm 5.45^b$ |
| Viscosity (cps)          | $46500 \pm 707.11^a$   | $68.75 \pm 8.84^b$ |
| Solubility (%)           | $32.12 \pm 0.53^b$     | $98.62 \pm 1.24^a$ |

Values are presented as mean  $\pm$  SD. Different superscripts correspond to significant differences ( $p < 0.05$ ) between values in each column.

### Changes in apparent viscosity and solubility

In this study, the use of  $\beta$ -mannanase in enzymatic hydrolysis resulted in a significant reduction in the apparent viscosity of PG by almost 700 times, from  $46500 \pm 707.11$  to  $68.75 \pm 8.84$  (**Table 1**). This

reduction in viscosity is attributed to the significant decrease in the MW of PG. As a high MW polymer, PG creates physically cross-linked dispersions through hydrogen bonds and entanglements when dissolved, leading to limited flowability and increased viscosity

levels [18]. Enzymatic hydrolysis breaks these hydrogen bonds, causing a decrease in MW and viscosity. A similar trend was observed in KG and other polysaccharides, including starch, carrageenan, and guar gum [38].

The solubility of PG increased significantly by 3 times from  $32.12 \pm 0.53$  to  $98.62 \pm 1.24$  % (**Table 1**). The presence of acetyl groups affects the solubility of glucomannan, which decreases during the deacetylation process [8]. However, this study found that the solubility of PGH increased despite removing the acetyl group during hydrolysis, as shown by the disappearance of the peak at  $2939$  and  $1734\text{ cm}^{-1}$  in the FTIR results (**Figure 2**). The hydrolysis process breaks down the hydrogen bonds between glucomannan molecules in aqueous solution, thus weakening the hydrogen bonds and neutralizing the effect of deacetylation [44]. This, in turn, leads to increased solubility in water. The reduction in MW can also contribute to the increase in solubility since less compact and more porous particles are typically more soluble [32]. As a result, despite the deacetylation, the solubility of PG still increases after the hydrolysis process in this study.

Glucomannan is widely recognized for its low solubility and high viscosity, which restricts its usage in industries such as food, pharmaceuticals, and health [16,17]. Nevertheless, by reducing its viscosity and enhancing its solubility, glucomannan's potential applications in these sectors can be extended.

### Oligosaccharides composition of PGH

An HPLC analysis was performed to determine the composition of PGH oligosaccharides. The analysis revealed 3 peaks: Mannohexaose, mannotriose, and mannobiose (**Figure 3**). Mannohexaose was found to be the most abundant, with an average value of  $141.39 \pm 8.09$  mg/g, followed by mannotriose at  $95.47 \pm 5.26$  mg/g and mannobiose at  $5.08 \pm 0.34$  mg/g (**Table 2**).  $\beta$ -mannanase is a type of hydrolase enzyme that can hydrolyze the  $\beta$ -1,4-mannosidic bonds in the main chain of glucomannan and produce straight or branched chain oligosaccharides of a certain length [45]. These findings were slightly different from the study conducted by Safitri *et al.* [22], which showed that hydrolysis of PG from porang flour produced oligosaccharides consisting of mannobiose, mannotriose, mannotetraose, and mannohexaose. On the other hand, hydrolysis of KG using  $\beta$ -mannanase produced oligosaccharides consisting of mannobiose, mannotriose, mannopentaose, and mannohexaose [46,47]. These dissimilar results indicated that different substrates produced different hydrolysate products. Importantly, this study found no presence of monosaccharides such as mannose or glucose in PGH, which is a desirable outcome as these are not the desired end products of glucomannan hydrolysis [48].

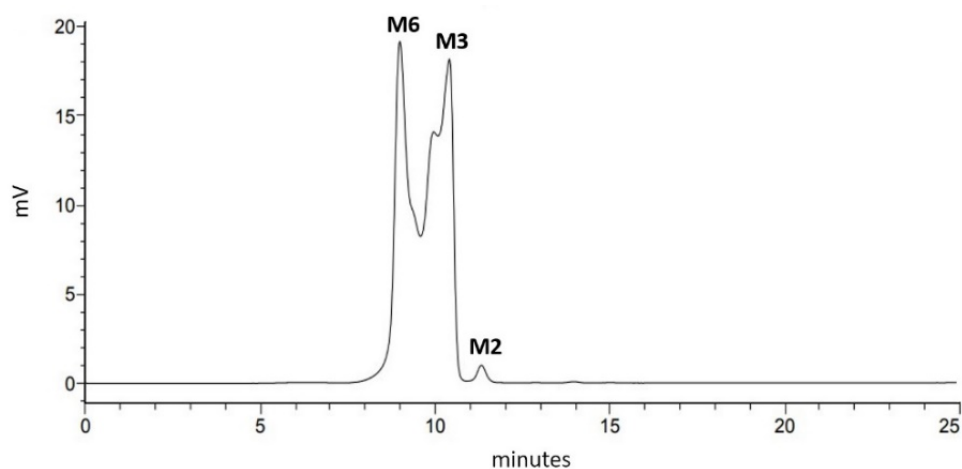


**Figure 3** HPLC profiles of oligosaccharides from hydrolysis of PG.

**Table 2** Oligosaccharide products from hydrolysis of PG.

| Oligosaccharides (mg/g) |              |             |                |  |
|-------------------------|--------------|-------------|----------------|--|
| M6                      | M3           | M2          | Total          |  |
| 141.39 ± 8.09           | 95.47 ± 5.26 | 5.08 ± 0.34 | 241.94 ± 10.54 |  |

### Growth of bacterial strains on different carbon sources

A prebiotic is defined as a substrate that is selectively utilized by host microorganisms, conferring a health benefit [49]. To determine whether a carbohydrate exhibits prebiotic activity, it must be metabolized as well, or nearly as well, as glucose by a specific probiotic strain [31]. Thus, the viable cells of

various Lactobacilli and Bifidobacteria were measured after 24 h of growth on a single carbon source of 2 % (w/v) glucose or samples of 2 % (w/v) PG or PGH, as well as 2 % (w/v) inulin as a comparison of commercial prebiotics. The same procedure was carried out to test the growth of *E. coli* FNCC 0091, selected to represent the enteric portion of the commensal flora. The results are shown in **Figure 4**.

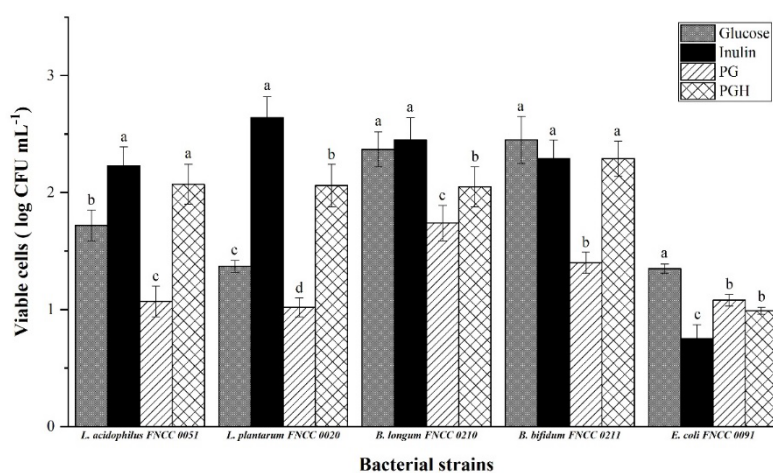


**Figure 4** Increases in viable cells presented as log (CFU mL<sup>-1</sup>) for bacterial strains grown in glucose, inulin, PG, and PGH for 24 h. Bars with different lowercase letters represent scores significantly different ( $p < 0.05$ ) for each bacterial strain.

The viable cell counts (log CFU mL<sup>-1</sup>) for *L. acidophilus* FNCC 0051 and *L. plantarum* FNCC 0020 were significantly higher when cultured in PGH compared to glucose. Conversely, the number of viable cells for *B. longum* FNCC 0210 was notably lower when grown in PGH than in glucose. Meanwhile, there was no significant difference in the number of viable cells for *B. bifidum* FNCC 0211 when grown in either PGH or glucose. Inulin also significantly increased the number of viable cells for all Lactobacilli compared to glucose, while no significant differences were observed in the number of viable cells of Bifidobacteria when cultivated on inulin or glucose. In contrast, PG resulted in a significantly lower increase in viable cells for all Lactobacilli and Bifidobacteria compared to glucose, inulin, and PGH.

Previous studies have demonstrated that hydrolyzed glucomannan has a greater ability to stimulate the growth of Lactobacilli and Bifidobacteria compared to unhydrolyzed glucomannan [16,20,21,50], which aligns with the findings of this study. The hydrolysis process breaks the hydrogen bonds in glucomannan, resulting in a hydrolysate with a simpler structure, much lower MW, and DP. This simpler structure allows for easier utilization by probiotic bacteria [20,51]. The absence of the acetyl group in PGH (**Figure 2**) may make it easier for Lactobacilli and Bifidobacteria to ferment it. Typically, oligosaccharides containing acetyl groups are fermented more slowly by fecal bacteria than those without acetyl groups [51]. In this study, PGH stimulated the growth of all bacterial strains nearly as effectively as inulin.

In addition to promoting the growth of probiotic bacteria, prebiotic substrates must be selective and cannot be fermented by commensal organisms. As depicted in **Figure 4**, the growth of *E. coli* FNCC 0091 on inulin, PG, and PGH was significantly lower than on glucose. This finding is consistent with several studies that found that enteric bacteria *E. coli* had less growth on prebiotic media than on media containing glucose [29,31,52].

### Prebiotic activity score

The prebiotic activity scores of inulin, PG, and PGH for Lactobacilli and Bifidobacteria (**Figure 5**) were calculated based on the viable cells (**Figure 4**) using Eq. (2). The highest prebiotic activity score of 1.37 was achieved by *L. plantarum* FNCC 0020 when grown on inulin, followed by *L. plantarum* FNCC 0020 grown on PGH, and *L. acidophilus* FNCC 0051 grown on inulin with scores of 0.77 and 0.75, respectively. Similar prebiotic activity scores were also observed with *L. acidophilus* FNCC 0051 grown on PGH, *B. longum* FNCC 0210, and *B. bifidum* FNCC 0211 grown in

inulin, with scores of 0.47, 0.48, and 0.39, respectively. *B. longum* FNCC 0210 and *B. bifidum* FNCC 0211 grown in PGH exhibited prebiotic activity scores that were not significantly different, with scores of 0.21 and 0.13, respectively.

In contrast to inulin and PGH, all strains exhibited negative prebiotic activity scores when grown on PG. This finding differs from earlier studies, which reported a positive prebiotic index of PG [19, 20]. This difference is likely due to previous research using PG extracted from porang flour, whereas, in this study, PG was directly extracted from the tubers, resulting in different characteristics. Moreover, previous studies employed fecal samples in the PG fermentation process, while our study utilized a single strain. The collaborative and interactive nature of different bacterial species in mixed fecal cultures may enhance polysaccharide utilization compared to pure bacterial cultures with limited polysaccharide-degrading enzymes [53]. Additionally, the addition of PG to the growth medium led to a high increase in viscosity, rendering it inaccessible to all bacterial strains.

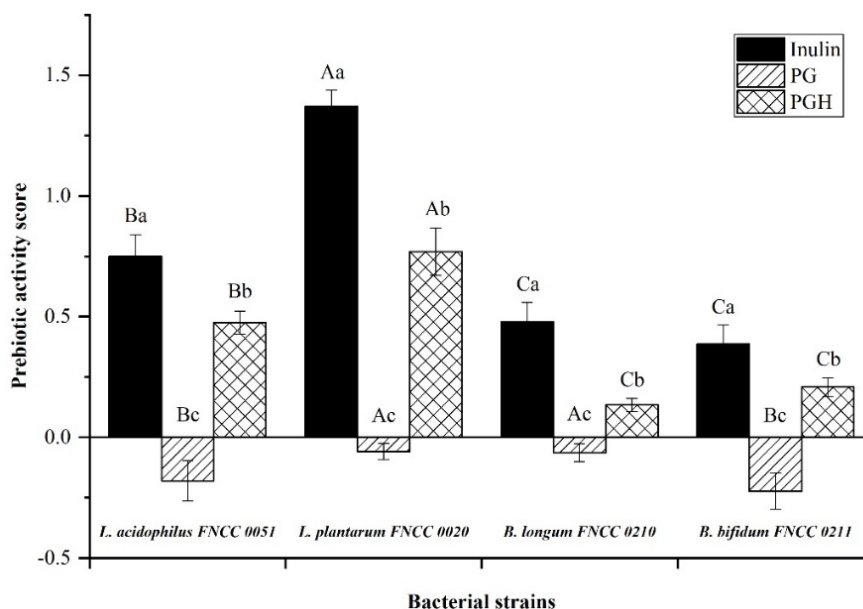


**Figure 5** Prebiotic activity scores of various bacterial strains grown on inulin, PG, and PGH. Bars with different capital letters represent scores significantly different ( $p < 0.05$ ) for each carbon source. Bars with different lowercase letters represent scores significantly different ( $p < 0.05$ ) for each bacterial strain.

PGH demonstrated a positive prebiotic activity score for all bacterial strains. This implies that PGH stimulated the growth of beneficial Lactobacilli and Bifidobacteria while selectively inhibiting the growth of

pathogenic *E. coli*. Notably, the prebiotic activity score of PGH was found to be higher in Lactobacilli than in Bifidobacteria, suggesting that Bifidobacteria are not strong fermenters of glucomannan hydrolysate [21,50].

It was also observed that the ability of Lactobacilli and Bifidobacteria to ferment PGH varied depending on the specific bacterial strain.

### Conclusions

Hydrolysis of PG extracted from fresh porang tubers resulted in the production of PGH, which consisted of 58 % mannohexaose, 40 % mannotriose, and 2 % mannobiose. PGH was characterized by examining its morphology, molecular structure, DP, MW, viscosity, and solubility. Subsequently, its prebiotic activity was evaluated *in vitro*. The findings revealed that hydrolysis caused damage to the PG granules and altered its molecular structure through the cleavage of glycosidic bonds and deacetylation. Additionally, the hydrolysis process significantly reduced the DP and MW of PG by 1000 times and 60 times, resulting in low viscosity ( $68.75 \pm 8.84$  cps) and high solubility ( $98.62 \pm 1.24$  %) of PGH. These characteristics make PGH more suitable for a broader range of food, pharmaceutical, and health products, especially in liquid form.

The prebiotic activity scores of PG were all negative, but they became positive after the hydrolysis process for all bacterial strains tested, indicating that PGH exhibited better prebiotic activity than PG. Further studies utilizing animal models may be necessary to better understand the prebiotic effects of PGH and its potential to modulate the gut microbiota.

### Acknowledgments

This study was supported by the Ministry of Research and Technology/National Research and Innovation Agency of the Republic of Indonesia (RISTEK-BRIN) through the research grant “Pendidikan Magister menuju Doktor untuk Sarjana Unggul (PMDSU) Batch III” with grant number 2970/UN1.DITLIT/DIT-LIT/LT/2019.

### References

- [1] RF Tester and FH Al-Ghazzewi. Glucomannan and nutrition. Mannans and health, with a special focus on glucomannans. *Food Research International* 2013; **50(1)**, 394-391.
- [2] R Tester and F Al-Ghazzewi. Glucomannan and nutrition. *Food Hydrocolloids* 2017; **68**, 246-254.
- [3] E Harmayani, V Aprilia and Y Marsono. Characterization of glucomannan from *Amorphophallus oncophyllus* and its prebiotic activity *in vivo*. *Carbohydrate Polymers* 2014; **112**, 475-479.
- [4] A Lopez-Rubio, P Tarancon, LG Gomez-Mascaraque, M Martinez-Sanz, MJ Fabra, JC Martinez and S Fiszman. Development of glucomannan-chitosan interpenetrating hydrocolloid networks (IHNs) as a potential tool for creating satiating ingredients. *Food Hydrocolloids* 2016; **60**, 533-542.
- [5] Y Zhang, C Tong, Y Chen, X Xia, S Jiang, C Qiu and J Pang. Advances in the construction and application of konjac glucomannan-based delivery systems. *International Journal of Biological Macromolecules* 2024; **262(1)**, 129940.
- [6] AA Anggraeni, P Triwitono, LA Lestari and E Harmayani. Evaluation of glucomannan as a fat replacer in the dough and cookies made from fermented cassava flour and soy protein concentrate. *Food Chemistry* 2024; **434**, 137452.
- [7] IWR Widarta, A Rukmini, U Santoso, Supriyadi and S Raharjo. Optimization of oil-in-water emulsion capacity and stability of octenyl succinic anhydride-modified porang glucomannan (*Amorphophallus muelleri* Blume). *Heliyon* 2022; **8(5)**, e09523.
- [8] B Azhar, S Gunawan, ERF Setyadi, L Majidah, F Taufany, L Atmaja and HW Aparamarta. Purification and separation of glucomannan from porang tuber flour (*Amorphophallus muelleri*) using microwave assisted extraction as an innovative gelatine substituent. *Heliyon* 2022; **9(11)**, e21972.
- [9] L Guo, HD Goff, M Chen and F Zhong. The hydration rate of konjac glucomannan after consumption affects its *in vivo* glycemic response and appetite sensation and *in vitro* digestion characteristics. *Food Hydrocolloids* 2022; **122**, 107102.
- [10] S Gurusmatika, K Nishi, E Harmayani, Y Pranoto and T Sugahara. Immunomodulatory activity of octenyl succinic anhydride modified porang (*Amorphophallus oncophyllus*) glucomannan on mouse macrophage-like J774.1 cells and mouse primary peritoneal macrophages. *Molecules* 2017;

- 22(7)**, 1187.
- [11] J Liu, Q Xu, J Zhang, X Zhou, F Lyu, P Zhao and Y Ding. Preparation, composition analysis and antioxidant activities of konjac oligo-glucomannan. *Carbohydrate Polymers* 2015; **130**, 398-404.
- [12] M Chua, K Chan, TJ Hocking, PA Williams, CJ Perry and TC Baldwin. Methodologies for the extraction and analysis of konjac glucomannan from corms of *Amorphophallus konjac* K. Koch. *Carbohydrate Polymers* 2012; **87(3)**, 2202-2210.
- [13] AC Kumoro, THA Yuganta, R Ratnawati and DS Retnowati. Effect of catalyst concentration and reaction time on the extraction of glucomannan from porang (*Amorphophallus oncophyllus*) flour via acid hydrolysis. *IOP Conference Series: Materials Science and Engineering* 2016; **162**, 012020.
- [14] A Yanuriati, DW Marseno, Rochmadi and E Harmayani. Characteristics of glucomannan isolated from fresh tuber of porang (*Amorphophallus muelleri* Blume). *Carbohydrate Polymers* 2017; **156**, 56-63.
- [15] DH Wardhani, JA Vazquez, DA Ramdani, A Lutfiati, N Aryanti and H Cahyono. Enzymatic purification of glucomannan from *Amorphophallus oncophyllus* using  $\alpha$ -amylase. *Bioscience Journal* 2019; **35(1)**, 277-288.
- [16] C Wang, P Lai, M Chen and H Chen. Antioxidative capacity produced by *Bifidobacterium*- and *Lactobacillus acidophilus*-mediated fermentations of konjac glucomannan and glucomannan oligosaccharides. *Journal of the Science of Food and Agriculture* 2008; **88(7)**, 1294-1300.
- [17] T Pan, S Peng, Z Xu, B Xiong, C Wen, M Yao and J Pang. Synergetic degradation of konjac glucomannan by  $\gamma$ -ray irradiation and hydrogen peroxide. *Carbohydrate Polymers* 2013; **93(2)**, 761-767.
- [18] Y Zhao, J Wang, Y Zhang, R He, Y Du and G Zhong. Hydration properties and mesoscopic structures of different depolymerized konjac glucomannan: Experiments and molecular dynamics simulations. *Food Hydrocolloids* 2024; **151**, 109853.
- [19] CA Ariestanti, V Seechamnaturakit, E Harmayani and S Wichienchot. Optimization on production of konjac oligo-glucomannan and their effect on the gut microbiota. *Food Science & Nutrition* 2019; **7(2)**, 788-796.
- [20] Anggela, E Harmayani, W Setyaningsih and S Wichienchot. Prebiotic effect of porang oligo-glucomannan using fecal batch culture fermentation. *Food Science and Technology* 2021; **42**, e06321.
- [21] A Dinoto, CC Watumlawar and Yopi. *In vitro* modulation of human intestinal microbiota by mannoglycosaccharides synthesized from *Amorphophallus muelleri* glucomannan. *Microbiology Indonesia* 2016; **7(4)**, 144-151.
- [22] AH Safitri, Yopi and A Meryandini. Enzymatic hydrolysis of porang by *Streptomyces violascens* BF 3.10 mannanase for the production of mannooligosaccharides. *Media Peternakan* 2014; **37(3)**, 143-214.
- [23] A Anggela, W Setyaningsih, S Wichienchot and E Harmayani. Oligo-glucomannan production from porang (*Amorphophallus oncophyllus*) by enzymatic hydrolysis using  $\beta$ -mannanase. *Indonesian Food and Nutrition Progress* 2020; **17(1)**, 23-27.
- [24] X Shi, J Yin, L Zhang, X Huang and S Ni. Studies on O-acetyl-glucomannans from *Amorphophallus* species: Comparison of physicochemical properties and primary structures. *Food Hydrocolloids* 2019; **89**, 503-511.
- [25] J Chen, D Liu, B Shi, H Wang, Y Cheng and W Zhang. Optimization of hydrolysis conditions for the production of glucomanno-oligosaccharides from konjac using  $\beta$ -mannanase by response surface methodology. *Carbohydrate Polymers* 2013; **93(1)**, 81-88.
- [26] I Ratcliffe, PA Williams, C Viebke and J Meadows. Physicochemical characterization of konjac glucomannan. *Biomacromolecules* 2005; **6(4)**, 1977-1986.
- [27] X Du, J Li, J Chen and B Li. Effect of degree of deacetylation on physicochemical and gelation properties of konjac glucomannan. *Food Research International* 2012; **46(1)**, 270-278.
- [28] J Rungruangsaphakun and S Keawsompong. Optimization of hydrolysis conditions for the

- mannooligosaccharides copra meal hydrolysate production. *3 Biotech* 2018; **8(3)**, 169.
- [29] J Huebner, RL Wehling and RW Hutkins. Functional activity of commercial prebiotics. *International Dairy Journal* 2007; **17(7)**, 770-775.
- [30] ES Rahayu, IH Rusdan, A Athennia, RZ Kamil, PC Pramesi, Y Marsono, T Utami and J Widada. Safety assessment of indigenous probiotic strain *Lactobacillus plantarum* Dad-13 isolated from dadih using Sprague Dawley rats as a model. *American Journal of Pharmacology and Toxicology* 2019; **14(1)**, 38-47.
- [31] S Zhang, H Hu, L Wang, F Liu and S Pan. Preparation and prebiotic potential of pectin oligosaccharides obtained from citrus peel pectin. *Food Chemistry* 2018; **244**, 232-237.
- [32] X Luo, X Yao, C Zhang, X Lin and B Han. Preparation of mid-to-high molecular weight konjac glucomannan (MHKGM) using controllable enzyme-catalyzed degradation and investigation of MHKGM properties. *Journal of Polymer Research* 2012; **19**, 989.
- [33] YR Herrero, KL Camas and A Ullah. *Characterization of biobased materials*. In: S Ahmed and Annu (Eds.). *Advanced applications of biobased materials: Food, biomedical, and environmental applications*. Elsevier Science, Amsterdam, Netherland, 2023.
- [34] ABD Nandiyanto, R Ragadhita and M Fiandini. Interpretation of fourier transform infrared spectra (FTIR): A practical approach in the polymer/plastic thermal decomposition. *Indonesian Journal of Science and Technology* 2023; **8(1)**, 113-126.
- [35] S Mahanta, J Shree, SC Santra, D Moulick and Akbar Hossain. *Deciphering of mycogenic nanoparticles by spectroscopic methods*. In: M Kuddus, IZ Ahmad and CM Hussain (Eds.). *Myconanotechnology and application of nanoparticles in biology: Fundamental concepts, mechanism and industrial applications*. Academic Press, Massachusetts, 2023.
- [36] RK Suryawanshi and N Kango. Production of mannoooligosaccharides from various mannans and evaluation of their prebiotic potential. *Food Chemistry* 2021; **334**, 127428.
- [37] P Tripetch, S Lekhavat, S Devahastin and C Borompichaichartkul. Antioxidant activities of konjac glucomannan hydrolysates of different molecular weights at different values of pH. *Foods* 2023; **12(18)**, 3406.
- [38] Y Li, H Liu, Y Xie, KI Shabani and X Liu. Preparation, characterization and physicochemical properties of konjac glucomannan depolymerized by ozone assisted with microwave treatment. *Food Hydrocolloids* 2021; **119**, 106878.
- [39] Y Zhang, Y Zhao, W Yang, G Song, P Zhong, Y Ren and G Zhong. Structural complexity of Konjac glucomannan and its derivatives governs the diversity and outputs of gut microbiota. *Carbohydrate Polymers* 2022; **292**, 119639.
- [40] T Hongbo, W Lan, L Yanping and D Siqing. Effect of acidolysis and oxidation on structure and properties of konjac glucomannan. *International Journal of Biological Macromolecules* 2019; **130**, 378-387.
- [41] Z Chen, S Wang, L Shang, P Zhou, J Li and B Li. An efficient and simple approach for the controlled preparation of partially degraded konjac glucomannan. *Food Hydrocolloids* 2020; **108**, 106017.
- [42] B Cai, X Yi, Q Han, J Pan, H Chen, H Sun and P Wan. Structural characterization of oligosaccharide from *Spirulina platensis* and its effect on the faecal microbiota *in vitro*. *Food Science and Human Wellness* 2022; **11(1)**, 109-118.
- [43] J Yin, L Ma, M Xie, S Nie and J Wu. Molecular properties and gut health benefits of enzyme-hydrolyzed konjac glucomannans. *Carbohydrate Polymers* 2020; **237**, 116117.
- [44] L Wang, G Huang, T Xu and J Xiao. Characterization of carboxymethylated konjac glucomannan for potential application in colon-targeted delivery. *Food Hydrocolloids* 2019; **94**, 354-362.
- [45] WHV Zyl, SH Rose, K Trollope and JF Gorgens. Fungal  $\beta$ -mannanases: Mannan hydrolysis, heterologous production and biotechnological applications. *Process Biochemistry* 2010; **45(8)**, 1203-1213.
- [46] M Zhang, X Chen, Z Zhang, C Sun, L Chen, H He, B Zhou and Y Zhang. Purification and functional

- characterization of endo- $\beta$ -mannanase MAN5 and its application in oligosaccharide production from konjac flour. *Applied Microbiology and Biotechnology* 2009; **83(5)**, 865-873.
- [47] J Liu, A Basit, T Miao, F Zheng, H Yu, Y Wang, W Jiang and Y Cao. Secretory expression of  $\beta$ -mannanase in *Saccharomyces cerevisiae* and its high efficiency for hydrolysis of mannans to mannoooligosaccharides. *Applied Microbiology and Biotechnology* 2018; **102**, 10027-10041.
- [48] W Xu, M Han, W Zhang, F Zhang, F Lei, K Wang and J Jiang. Production of manno-oligosaccharide from *Gleditsia microphylla* galactomannan using acetic acid and ferrous chloride. *Food Chemistry* 2021; **346**, 128844.
- [49] GR Gibson, R Hutkins, ME Sanders, SL Prescott, RA Reimer, SJ Salminen, K Scott, C Stanton, KS Swanson, PD Cani, K Verbeke and G Reid. The International Scientific Association for Probiotics and Prebiotics (ISAPP) consensus statement on the definition and scope of prebiotics. *Nature Reviews Gastroenterology & Hepatology* 2017; **14(8)**, 491-502.
- [50] J Yang, N Vittori, W Wang, Y Shi, JL Hoeflinger, MJ Miller and Y Pan. Molecular weight distribution and fermentation of mechanically pre-treated konjac enzymatic hydrolysates. *Carbohydrate Polymers* 2017; **159**, 58-65.
- [51] F Li, X Sun, W Yu, C Shi, X Zhang, H Yu and F Ma. Enhanced konjac glucomannan hydrolysis by lytic polysaccharide monoxygenases and generating prebiotic oligosaccharides. *Carbohydrate Polymers* 2021; **253**, 117241.
- [52] ME Kustyawati, ME Nurlita, EG Fadhallah and S Rizal. Prebiotic activity of *Lactobacillus casei* grown on medium containing *Hylocereus undatus* extract and its use in the fermentation of goat's milk kefir. *Biodiversitas Journal of Biological Diversity* 2022; **23(12)**, 6513-6519.
- [53] A Song, Y Mao, K Siu and J Wu. Bifidogenic effects of *Cordyceps sinensis* fungal exopolysaccharide and konjac glucomannan after ultrasound and acid degradation. *International Journal of Biological Macromolecules* 2018; **111**, 587-594.